

# Varactor Properties for Wide-Band Linear-Tuning Microwave VCO's

DEAN F. PETERSON, MEMBER, IEEE

**Abstract**—Varactor properties and a particular hyperabrupt doping profile are identified which can provide wide-band tuning linearity for an important class of microwave oscillators. The results are most appropriate for series-tuned oscillators realized with simple configurations of BJT's or FET's in chip, integrated, or monolithic form with low parasitics. The derivation for the doping profile is presented and includes the effects of large signals in modifying the effective varactor capacitance. In addition, breakdown conditions and the level and variation in series resistance are included. When the results are applied to BJT and FET oscillator circuits with measured large-signal properties, the profiles obtained predict excellent linearity for the FET over a 7-12-GHz frequency range and fair linearity for the BJT circuit from 2 to 4 GHz. The profiles are reasonable and should be realizable with existing varactor fabrication technology.

## I. INTRODUCTION

VOLTAGE controlled oscillators (VCO's) are important components in a variety of microwave systems. In many applications, particularly ECM, system performance is greatly facilitated when these oscillators are capable of wide tuning bandwidths with linear voltage-to-frequency tuning as well as high-speed frequency switching. The use of varactor tuning allows high speed while affording small size and up to octave bandwidths [1]–[5]. Furthermore, the development of “hyperabrupt” tuning varactors has provided improvements in tuning linearity over half-octave bandwidths [6]. In addition to the use of tuning varactors with wide capacitive variations, methods of improving tuning range utilizing circuit reactance compensation has been successful in cases where device and varactor packaging parasitics are visible [7]–[9].

With the development and continued improvement in microwave FET's and BJT's, in addition to the Gunn-effect device, wide-band varactor tuned oscillators (VTO's) can be realized in chip form as integrated and possibly monolithic circuits in simple configurations. Particularly, the three-terminal devices can be used in a manner which provides separate ports for tuning and output power such that the tuning-port impedance is low and active over a wide bandwidth to allow wide tuning ranges. In these circuits, the nature of the impedance under small and large signals at the tuning port behaves in a way which suggests simple, minimum stored energy

tuning circuitry with chip varactors and identifies appropriate varactor capacitance characteristics for linear tuning over wide (octave) bandwidths. The common nature of these equivalent active circuits (including Gunn devices) allows a particular form of varactor doping profile to be useful with these devices in accomplishing linearity.

The purpose of this paper is to derive, utilizing the observed nature of simple FET and BJT oscillator circuits, chip tuning varactor characteristics for achieving tuning linearity over wide bandwidths in the frequency range of 2 to approximately 20 GHz. In developing these characteristics, the nonlinear effects of large signals in the varactor and active device are taken into account by use of the describing function concept [10]. The theory applies in the case when the RF current in the tuning varactor is essentially single frequency, or often equivalently, if the oscillator is essentially series tuned. In Section II, the basic theory is developed and the varactor properties and doping profile are derived. The theory is applied to FET and BJT oscillator circuits with measured tuning-port large-signal impedance characteristics in Section III, and appropriate doping profiles are identified. Excellent linearity for a 7-12-GHz FET oscillator is predicted, while that for a 2-4-GHz BJT oscillator is less impressive.

## II. VARACTOR PROPERTIES FOR TUNING LINEARITY WITH A CLASS OF MICROWAVE OSCILLATORS

### A. Circuit Model

The performance and limitations of varactor-tuned VCO's can often be obtained by studying the interaction between the tuning element (varactor) and its equivalent one-port nonlinear active terminating network as shown in Fig. 1. This viewpoint can lead to specification of the nature of the active terminating network to achieve widest tuning, can identify properties of the varactor for voltage-to-frequency tuning linearity, and can specify the dynamical behavior of the natural frequency and amplitude of oscillation [11].

Under oscillation conditions, the interaction of the device and varactor nonlinearities can result in non-sinusoidal voltages and currents in the circuit, complicating the problem of varactor specification. To account for large-signal effects in a varactor and develop appropriate doping profiles for linear tuning VTO's, the nature of the large signal must be known or assumed. Any assumption

Manuscript received August 20, 1979. This work was supported by Omni Spectra under Grant DRDA 79-775-C1, Omni Spectra Subcontract A61292-2, and by the Wright-Patterson Air Force Base under Prime Contract F33615-76-C-1189.

The author is with the Electron Physics laboratory, Department of Electrical and Computer Engineering, University of Michigan, Ann Arbor, MI 48109.

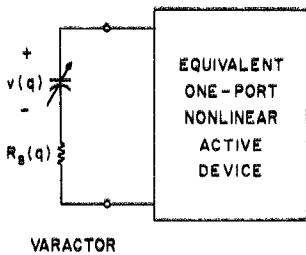


Fig. 1. Circuit model for studying varactor and active circuit interactions.

regarding the form of the large signal must obviously have a high degree of self-consistency when the actual tuning varactor is placed in the circuit. From a practical standpoint, most wide-band VTO's, particularly from 2 to 20 GHz, tend to be *series* tuned because of the nature of the active device series equivalent circuit and the difficulty of providing the normally small parallel-tuning inductances otherwise required. Since series-tuned circuits tend to suppress harmonics above the fundamental, it will be assumed that the RF current through the varactor is essentially sinusoidal, i.e.,

$$i(t) = -I_1 \sin \omega t. \quad (1)$$

The analysis given here applies to any oscillator in which (1) is valid, so that "series tuned" and "single-frequency current" are used synonymously.

### B. Varactor Model and Description

For the series-tuned case, the varactor can be characterized by a voltage-charge relation such as

$$v = f(q) + R_s(q) \frac{dq}{dt} \quad (2)$$

where

$$i = \frac{dq}{dt} \quad (3)$$

and where  $v$  is the total voltage across the varactor, comprised of a depletion layer voltage  $f(q)$  dependent on removed charge  $q$  and a resistive drop across a charge-variable series resistance  $R_s(q)$ . Since  $i(t)$  is sinusoidal,  $q(t)$  can be written as

$$q(t) = Q_0 + Q_1 \cos \omega t \quad (4)$$

where

$$I_1 = \omega Q_1. \quad (5)$$

Note that if harmonic currents are negligible, then harmonic charge amplitudes are further reduced by the harmonic number, and (4) is really the important assumption in the analysis.

Substituting (4) into (2) now gives

$$v(t) = \sum_{k=0}^{\infty} F_k(Q_0, Q_1) \cos k \omega t - I_1 \sum_{k=1}^{\infty} R_{sk}(Q_0, Q_1) \sin k \omega t \quad (6)$$

where

$$F_k(Q_0, Q_1) = \frac{1}{\pi} \int_0^{2\pi} f(Q_0 + Q_1 \cos \theta) \cos k \theta d\theta \quad (7a)$$

and

$$R_{sk}(Q_0, Q_1) = \frac{1}{\pi} \int_0^{2\pi} R_s(Q_0 + Q_1 \cos \theta) \sin \theta \sin k \theta d\theta. \quad (7b)$$

Hence, the dc voltage  $V_0$  across the varactor is given by

$$V_0 = F_0(Q_0, Q_1) \quad (8a)$$

and the fundamental voltage amplitude  $V_1$  can be written in complex form as

$$V_1 = F_1(Q_0, Q_1) + j\omega Q_1 R_{s1}(Q_0, Q_1). \quad (8b)$$

From (8b), the fundamental impedance  $Z_1$  of the varactor is

$$Z_1 = \frac{V_1}{j\omega Q_1} = R_{s1}(Q_0, Q_1) + \frac{S_1(Q_0, Q_1)}{j\omega} \quad (9)$$

where

$$S_1 = \frac{V_1}{Q_1} = \frac{F_1(Q_0, Q_1)}{Q_1} \quad (10)$$

is the fundamental tuning elastance. Since  $V_0$  is the same as the tuning voltage and is an independent variable, (8a) can be used to eliminate  $Q_0$  in (8b) and result in an expression for  $S_1$  in terms of  $V_0$  and  $Q_1$ .

### C. Varactor-Circuit Interaction

In the series-tuned oscillator with the RF current as given in (1), the equivalent one-port active device at the varactor terminals can be characterized by the single-frequency describing function  $Z_d(\omega, I_1)$ , where

$$Z_d(\omega, I_1) = R_d(\omega, I_1) + jX_d(\omega, I_1). \quad (11)$$

For oscillation at  $\omega$  using a varactor,

$$R_v + R_d(\omega, I_1) = 0 \quad (12a)$$

and

$$\frac{S_v}{\omega} = X_d(\omega, I_1) \quad (12b)$$

where  $R_v$  is the varactor effective series resistance and  $S_v$  is the required tuning varactor elastance. The RF-current amplitude is determined from (12a), and (12b) then specifies  $S_v$  for oscillation at  $\omega$  with amplitude  $I_1$ . If it is desired to tune the oscillator from  $\omega_1$  to  $\omega_2$ , then (12) determines the required behavior of  $S_v[\omega, I_1(\omega)]$ ,  $\omega_1 < \omega < \omega_2$ , and this information can be used to obtain an appropriate varactor with  $S_1 = S_v$  and  $R_v = R_{s1}$  at tuning voltages linearly related to  $\omega$ . Initially  $R_v$  and hence  $R_{s1}$  will be assumed approximately constant. Appropriate modifications can be made if this is not the case.

The actual behavior of  $S_v$  over the tuning band can be varied somewhat by deliberate modification of the character of  $X_d$  by circuit changes. Based on the behavior of  $X_d$ , there will be some minimum variation required of  $S_v$  to accomplish the desired tuning ranges. This limitation can be deduced from (12b) by examining the differential of  $S_v/\omega^2$ , i.e.,

$$\frac{d}{d\omega} \left( \frac{S_v}{\omega^2} \right) = \frac{d}{d\omega} \left( \frac{X_d}{\omega} \right) \quad (13)$$

shows that the rate of change of the quantity  $S_v/\omega^2$  is independent of any linear series inductance in  $X_d$ . Since most active devices tend to be capacitive in nature thereby requiring the addition of series-tuning inductance for oscillation with a varactor, these capacitive effects determine the minimum value of the left-hand side of (13). Since the right-hand side of (13) is almost always positive,<sup>1</sup> then

$$\frac{d}{d\omega} \left( \frac{S_v}{\omega^2} \right) \geq 0 \quad (14)$$

and to tune from  $\omega_1$  where  $S_v = S_{\min}$  to  $\omega_2$  where  $S_v = S_{\max}$  would require

$$\beta = \frac{S_{\max}}{S_{\min}} = \frac{C_{\max}}{C_{\min}} \geq \left( \frac{\omega_2}{\omega_1} \right)^2. \quad (15)$$

It is possible for  $(d/d\omega)(X_d/\omega)$  to be negative by the use of reactance compensation [7]–[9]. Such compensation can be achieved over moderate bandwidths (less than an octave) with the consequence of additional frequency variation in  $R_d(\omega, I_1)$ , and increased reactance slopes out of band and additional stored energy. It is not considered here, since it would destroy the typical, simple nature of  $X_d(\omega)$  such that some degree of generality regarding tuning varactors would not be possible. For a given  $X_d(\omega)$ , the varactor requirements can be obtained by integration of (13) from  $\omega_1$  to  $\omega_2$ , to give, after rearrangement:

$$C_{\max} = \frac{\beta - \left( \frac{\omega_2}{\omega_1} \right)^2}{\omega_2^2 \left[ \frac{X_d(\omega_2)}{\omega_2} - \frac{X_d(\omega_1)}{\omega_1} \right]}. \quad (16)$$

This result indicates that values of  $\beta$  near  $(\omega_2/\omega_1)^2$  are possible if  $C_{\max}$  is small, and the tuning varactor impedance level is high. In this case the finite device capacitive effects apparent in the denominator of (16) are made negligible by the addition of a large series-tuning inductance. Of course, such a solution has a large amount of associated stored energy which can substantially increase oscillator recovery times from a nonequilibrium situation [11]. On the other hand, a large  $\beta$ , while reducing stored energy, makes the varactor rather ineffective as a tuning element. For octave-band tuning, a reasonable compromise occurs for values of  $\beta$  around 10. The tradeoffs between  $C_{\max}$  and  $\beta$  in (16) can be quickly established for a given device, without regard to the nature of  $X_d(\omega)$ , to arrive at the most desirable or achievable varactor characteristic.

#### D. Varactor Requirements for Linearity

To achieve linear voltage to frequency tuning, then

$$\omega(V_t) = \alpha V_t + \Omega \quad (17)$$

where  $V_t$  is the tuning voltage and  $\alpha$  and  $\Omega$  are constants. Hence the problem is to find a nonlinear function  $f(q)$

<sup>1</sup>If  $X_d$  were totally linear and the reactance of a lossless circuit element, then by Foster's Reactance Theorem,  $d/d\omega(X_d/\omega) \geq 0$  always.

such that

$$V_t + \gamma = V_0 = F_0(Q_0, Q_1) \quad (18a)$$

and

$$S_1(Q_0, Q_1) = S_v[\omega(V_t)] \quad (18b)$$

where

$$Q_1 = \frac{I_1[\omega(V_t)]}{\omega(V_t)} \quad (18c)$$

for each  $\omega(V_t)$ ,  $\omega_1 < \omega < \omega_2$ , where  $\gamma$  is a constant. In the general case, there is no guarantee that such a function exists for a given  $Q_1(\omega)$  and specified tuning voltage range. It is appropriate to treat the situation as an approximate problem by specifying a smoothly continuous nonlinear function and determining how closely it comes to the desired large-signal behavior and linearity. The approach taken here is to specify an appropriate form of the nonlinearity to within constants which can be adjusted to achieve best linearity. A function capable of giving good results for series-tuned microwave VTO's is the one which has an incremental capacitance  $C(v)$  given by

$$C(v) = \frac{dq}{dv} = \frac{1}{a + bv + cv^2}, \quad b^2 - 4ac > 0 \quad (19)$$

where  $a$ ,  $b$ , and  $c$  are adjustable positive constants and  $v > 0$  is the voltage across the varactor. This form arises from the nature of  $X_d(\omega, I_{RF})$  in series-tuned oscillators. Under small-signal conditions,  $X_d(\omega, I_{RF} \rightarrow 0)$  typically behaves as

$$X_d(\omega, I_{RF} \rightarrow 0) \approx \omega L_t - \frac{1}{\omega C_d} \quad (20)$$

where  $L_t$  is the required tuning inductance and  $C_d$  characterizes the usual capacitive behavior of the device. This behavior will be apparent in the experimental section. If the oscillator worked at small-signal levels, then from (20) and (12),

$$S_v = \omega^2 L_t - 1/C_d \quad (21)$$

and the tuning linearity requirement (17) shows that  $S_v$  will be quadratic in  $V_t$ , and  $C(v = V_t)$  will be as in (19). Under large-signal conditions, the device usually retains its capacitive nature such that  $a$ ,  $b$ , and  $c$  in (19) can be adjusted to obtain excellent tuning linearity.

To optimize linearity for a given active device, the function  $f(q)$  and the components  $F_0$  and  $F_1$  in (8) must be found for the  $C(v)$  in (19). Integration of (19) gives

$$q = \int C(v) dv = \frac{1}{d} \ln \frac{2cv + b - d}{2cv + b + d} \quad (22)$$

where

$$d = \sqrt{b^2 - 4ac} \quad (23)$$

and the constant of integration has been set to zero with no loss of generality. Solving (22) for  $v(q)$  gives

$$v(q) = -\frac{b}{2c} + \frac{d}{2c} \frac{1 + e^{dq}}{1 - e^{dq}}. \quad (24)$$

Now for  $q = Q_0 + Q_1 \cos \omega t$ ,  $F_0$  and  $F_1$  can be found as (see

## Appendix

$$F_0(Q_0, Q_1) = -\frac{b}{2c} + \frac{d}{2c} \left[ 1 + 2 \sum_{n=1}^{\infty} e^{ndQ_0} I_0(ndQ_1) \right] \quad (25a)$$

and

$$F_1(Q_0, Q_1) = \frac{d}{2c} \left[ 4 \sum_{n=1}^{\infty} e^{ndQ_0} I_1(ndQ_1) \right] \quad (25b)$$

where  $I_0(x)$  and  $I_1(x)$  are modified Bessel functions of orders 0 and 1, respectively, and argument  $x$ .

When it is assumed that  $S_v(\omega)$  and the corresponding  $Q_1(\omega)$ ,  $\omega_1 < \omega < \omega_2$ , are specified, linearity is optimized by first setting  $F_1$  equal to  $S_v Q_1$  in (25), i.e.,

$$S_v(\omega) Q_1(\omega) = \frac{d}{2c} \left[ 4 \sum_{n=1}^{\infty} e^{ndQ_0} I_1(ndQ_1(\omega)) \right] \quad (26)$$

which for a given  $d$  and  $c$  determines values for  $\exp[dQ_0(\omega)]$ . These values are then substituted into (25a) which determines  $F_0(\omega)$  to within a constant  $b/2c$ . Then  $F_0(\omega) + b/2c$  is fit to a best straight line in  $\omega$  in the minimax sense, thereby giving a measure of tuning linearity since  $F_0$  is the same as the tuning voltage. The values of  $d$  and  $c$  are adjusted to minimize the maximum deviation from a best straight line for various tuning voltage ranges. Having an optimum solution, the value of  $b$  is obtained by requiring that the minimum value of  $v$  in (24) under operating conditions be equal to zero. This will prevent forward bias in actual operation.

## E. Varactor Doping Profile

The doping profile of a one-dimensional one-sided varactor can be found in the usual way from  $C(v)$  in (19) as

$$N(W) = \frac{\epsilon}{e} \frac{1}{W} \frac{dv}{dW} \quad (27)$$

where  $N(W)$  is the doping level at a distance  $W$  from the junction and where  $\epsilon$  and  $e$  are the dielectric constant and electronic charge, respectively. Since

$$C(v) = \frac{\epsilon A}{W(v)} \quad (28)$$

where  $A$  is the device area,  $v(W)$  can be found from (19) and  $dv/dW$  calculated to give

$$N(W) = \frac{1}{eAW} \frac{1}{\sqrt{d^2 + 4cW/\epsilon A}}. \quad (29)$$

If

$$N_0 = \frac{4c}{\epsilon e A^2 d^3} \quad (30a)$$

$$W_0 = \epsilon A \frac{d^2}{4c} \quad (30b)$$

and

$$W' = W/W_0 \quad (30c)$$

then

$$N(W') = \frac{N_0}{W'(1+W')^{1/2}}. \quad (30d)$$

The profile must extend from  $W_{\min} = \epsilon A/C(0) = \epsilon Aa$  to  $W_{\max}$  determined by the maximum voltage ever present across the varactor at large-signal operating conditions.

Given optimum values of  $a$ ,  $b$ , and  $c$  for a particular situation, the area can be chosen to give an appropriate doping level or depletion-layer width. In determining a value for  $A$ , diode breakdown and the level of series resistance must be considered. In particular, the diode must not breakdown for  $W < W_{\max}$  and the change in varactor series resistance caused by depletion-layer variation should be small compared to  $R_{s1}$  if the assumption of constant  $R_{s1}$  is to be valid. There may be, of course, some situations where a variable  $R_{s1}$  would be advantageous in improving tuning linearity. However, to utilize this variation, all other sources of series resistance must be very well controlled.

The maximum electric field  $E_{\max}$  when  $W = W_{\max}$  is given by

$$E_{\max} = \Delta E + \frac{1}{\epsilon Ad} \ln \frac{\sqrt{1+W'_{\max}} - 1}{\sqrt{1+W'_{\max}} + 1} \frac{\sqrt{1+W'_{\min}} + 1}{\sqrt{1+W'_{\min}} - 1} \quad (31)$$

where

$$\Delta E = \frac{e}{\epsilon} \int_0^{W_{\min}} N(x) dx$$

and  $W'_{\max} = W_{\max}/W_0$ ,  $W'_{\min} = W_{\min}/W_0$ . Since the electric field falls rapidly above  $W_{\min}$  and at breakdown most of the ionization will be near  $E_{\max}$ , the breakdown conditions can be found with sufficient accuracy by considering an equivalent uniform profile of doping  $N_B$ , where

$$N_B = \frac{\epsilon}{e} \frac{dE}{dx} \Big|_{x=0} = N(0). \quad (32)$$

If it is assumed that

$$N(0) \approx \frac{N_0}{W'_{\min}(1+W'_{\min})^{1/2}} = N_B \quad (33)$$

then the relation between  $E_{\max}$  and  $N_0$  at breakdown can be found as in [12]. Only those solutions for  $N_0$  and/or  $A$  are possible if the resulting  $E_{\max}$  lies below the breakdown field at the effective doping  $N_B$ . Within this confinement, the component of series resistance  $\Delta R_s$  associated with the bulk material from  $W_e$  to  $W_{\max}$  should be made appropriately small, where  $W_e$  is the effective depletion-layer width at the minimum static-tuning voltage. For this profile,  $\Delta R_s$  is given by

$$\Delta R_s = \frac{\epsilon}{e\mu} \frac{d^2}{4cN_0} \left[ \frac{2}{15} (1+W'_{\max})^{3/2} (3W'_{\max} - 2) - \frac{2}{15} (1+W'_e)^{3/2} (3W'_e - 2) \right] \quad (34)$$

where  $\mu$  is the carrier mobility and  $W'_e = W_e/W_0$ .

### III. APPLICATION TO FET AND BJT OSCILLATORS

#### A. Oscillator Circuits

The theory is now used to determine appropriate varactor profiles for two VTO circuits, a BJT oscillator in the 2-4-GHz range and an FET oscillator from 7 to 12 GHz. The circuit diagrams for these FET oscillators are shown in Fig. 2, with the FET (Fig. 2(a)) operating in the common drain configuration tuned at the gate, and the BJT (Fig. 2(b)) operating common collector with the tuning in the base circuit. Both oscillators are effectively series tuned with the varactor  $R_s$  setting the saturation level and output power at the load port. For both of these circuits, the nonlinear behavior of the active device at the tuning port must be known for an appropriate tuning varactor to be defined. For both circuits, large-signal measurements were made at several frequencies and the resulting information was used in the analysis. Loading conditions on the output port were adjusted to provide at the tuning port an appropriate amount of negative resistance for varactor tuning over the frequency range of interest. Also, the relation between the output power and the RF-current level at the tuning port was measured for use in predicting output level across the band.

#### B. FET Oscillator

The large-signal impedance of the FET circuit at several frequencies is shown in Fig. 3. As can be seen, the reactive portion is capacitive and can be accurately represented by a series  $LC$  circuit, with  $C$  the nonlinear gate capacitance and  $L$  representing series lead inductance. As the capacitance increases with RF level, the negative resistance saturates, one reason being the decrease in the parameter  $g_m/C_g$ , where  $g_m$  is the FET transconductance.

To obtain a varactor profile for the FET oscillator, a constant load resistance of  $2 \Omega$  was assumed, thereby determining the operating RF current levels (12a) at each frequency as shown in Fig. 3(a). This resistance would be obtained as the varactor series resistance. Based on these current levels, the operating device reactances at the various frequencies are now determined to within a constant series-tuning inductance  $L_t$  for use in (12b). The value of  $L_t$  is determined by a specification of the maximum tuning capacitance ratio  $\beta$  in (16). In the following analysis, the results were obtained for  $\beta = 10$ , or  $L_t = 1.56 \text{ nH}$ . The optimizations were carried out only at the six frequencies where measured data was available.

Optimal solutions were generated by assuming a value of  $d$  in (26) and iterating the value of  $c$  until the maximum deviation  $\delta$  given by

$$\delta = (\max \delta_k) / \Delta V \quad (35)$$

with

$$\delta_k = \left| F_0(\omega_k) + \frac{b}{2c} - (k_1 \omega_k + k_2) \right|, \quad k = 1, 2, \dots, N \quad (36)$$

is a minimum, where  $k_1$  and  $k_2$  are always chosen for a

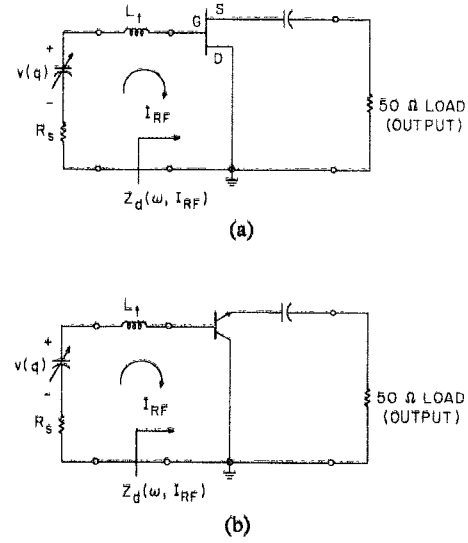


Fig. 2. Typical broad-band (a) FET; (b) BJT VTO circuits.

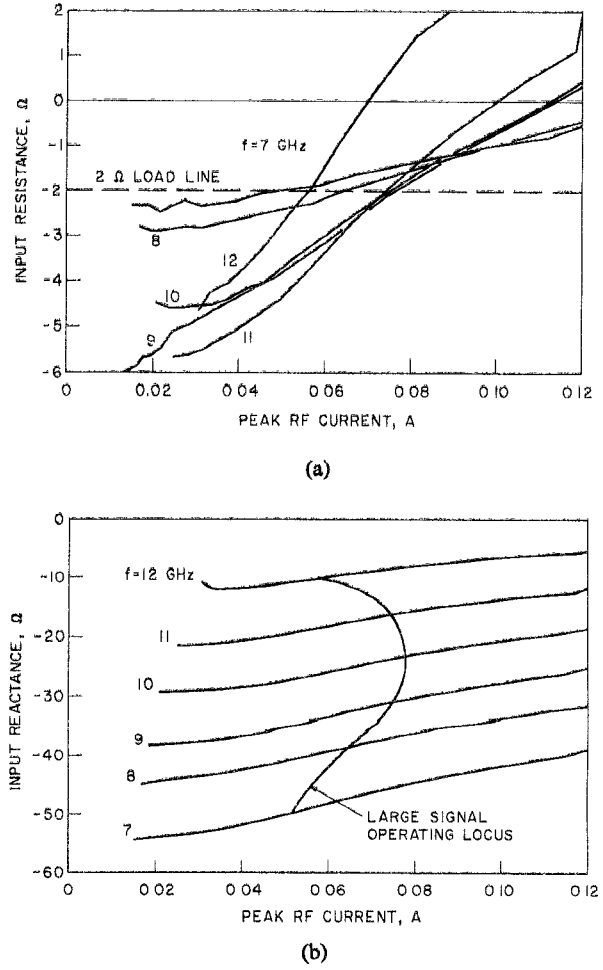


Fig. 3. Measured large-signal impedance of an NEC 695 common-drain oscillator circuit showing the effective operating conditions. (a)  $R_d(\omega, I_1)$ . (b)  $X_d(\omega, I_1)$ .

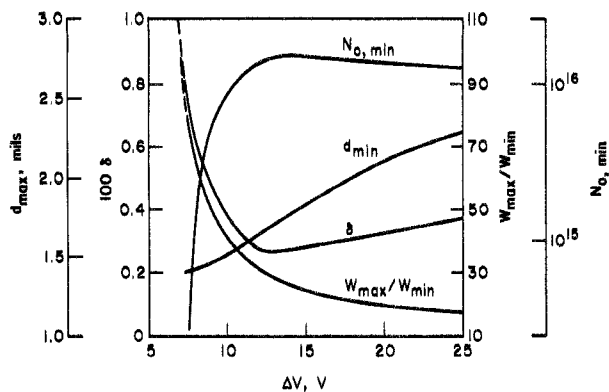


Fig. 4. Tuning linearity and varactor requirements for the FET oscillator circuit.

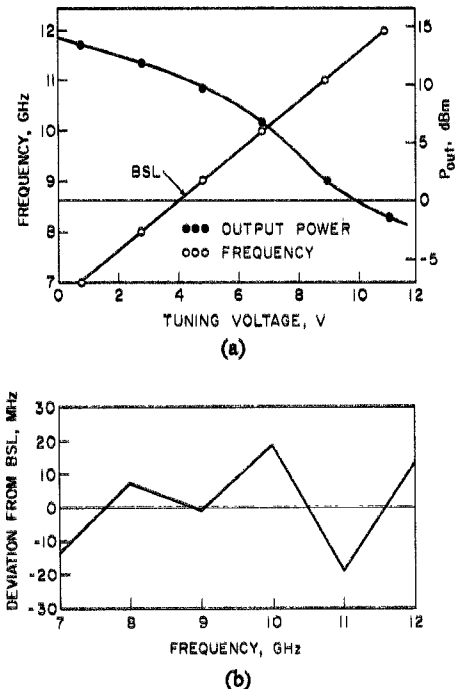


Fig. 5. (a) Tuning curve and output power. (b) Deviation from a BSL for the FET oscillator with  $\Delta V = 10$  V.

minimax solution,  $N$  is the number of frequencies, and  $\Delta V$  is the net change in tuning voltage, i.e.,  $\Delta V = F_0(\omega_N) - F_0(\omega_1)$ . The parameter  $\delta$  as a function of  $\Delta V$  for the FET oscillator is shown in Fig. 4, which displays a minimum value near  $\Delta V \approx 13$  V. Also indicated are the corresponding variations in  $W_{\max}/W_{\min}$ ,  $N_{0,\min}$ , and  $d_{\max}$ , where  $N_{0,\min}$  is the minimum doping level when  $\Delta R = 2 \Omega$  and  $d_{\max}$  is the maximum device diameter at  $N_{0,\min}$  (24a). It is evident that the best solutions from device diameter and  $W_{\max}/W_{\min}$  considerations are at high values of  $\Delta V$ , with only a small penalty in  $\delta$ . Most VTO designers, however, prefer tuning ranges of approximately 10 V since these changes can be readily achieved with high-speed digital circuitry or FET switches. For a  $\beta$  of 7, the values of  $\delta$  increase approximately 30 percent.

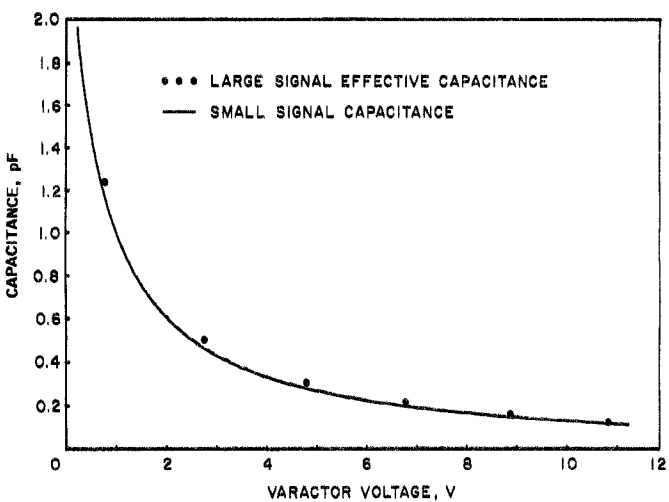


Fig. 6. Small signal  $CV$  characteristics and effective large-signal capacitance for the FET tuning varactor.

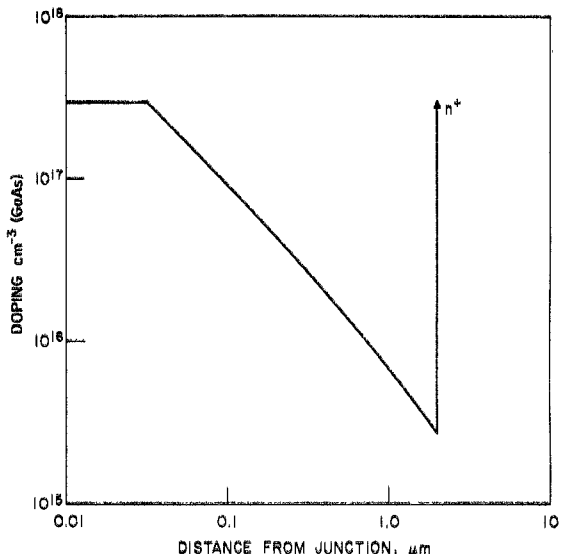


Fig. 7. Doping profile for the FET tuning varactor having the  $CV$  characteristic of Fig. 6,  $N_0 = 10^{16} \text{ cm}^{-3}$ .

The tuning linearity, output power<sup>2</sup> and deviation from a best straight line for a tuning range of 10 V are shown in Fig. 5. The peak deviation observed is approximately 20 MHz over the 7–12-GHz frequency range. With the indicated offset of approximately 0.8 V, the operating voltage at large signals will always exceed zero. Shown in Fig. 6 are the small-signal capacitance–voltage characteristic as well as the effective large-signal capacitance, indicating the amount of expansion under operating conditions. An appropriate doping profile to achieve the required tuning varactor characteristic is shown in Fig. 7, where  $N_0 = 10^{16} \text{ cm}^{-3}$ ,  $W_0 = 0.952 \mu\text{m}$ ,  $W_{\min} = 0.045 \mu\text{m}$ ,  $W_{\max} = 1.9$

<sup>2</sup>The output power is determined from the measured relation of RF current in the tuning loop to output power at the various frequencies.

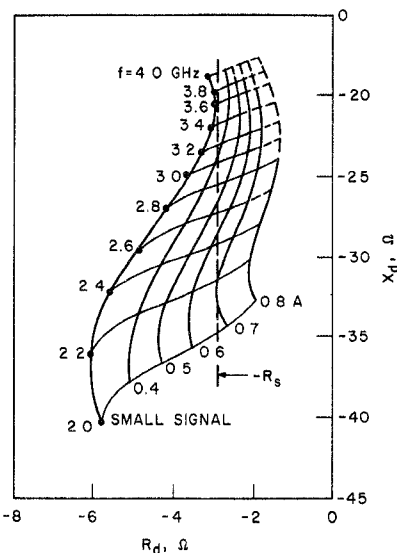


Fig. 8. Measured large-signal impedance of an NEC 220 BJT from 2 to 4 GHz. A constant  $R$  load line of  $2.9 \Omega$  was assumed.

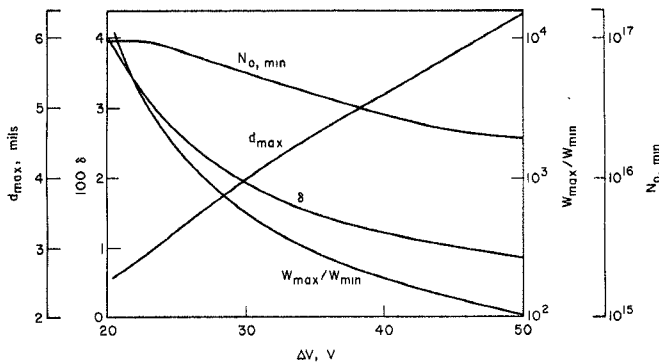


Fig. 9. Tuning linearity and varactor requirements for the BJT oscillator circuit.

$\mu\text{m}$ , and the device diameter is 1.47 mil. The variation in the large-signal  $R_{s1}$  based on the doping profile was  $0.23 \Omega$  which is deemed acceptable. This variation could be reduced for a larger  $N_0$  at the expense of device area. For this case  $N_B = 20.6$ ,  $N_0 = 2.06 \times 10^{17} \text{ cm}^{-3}$ , and the breakdown voltage is approximately 55 V. This is above the varactor voltage at  $W_{\max}$ , as required. It is evident that good tuning linearity should be achievable with the FET oscillator and the given tuning varactor.

#### C. BJT Oscillator

The measured impedance characteristics at the tuning port of the BJT oscillator are shown in Fig. 8 including a  $2.9\Omega$  load line for establishing steady-state operating currents. It is apparent that the operating current levels are approximately an order of magnitude higher over the 2–4-GHz range than those of the FET in the 7–12-GHz range. This is because the BJT is a higher power device by roughly a factor of ten. Based on the operating current levels (charges) and reactances, the required tuning elasticances were calculated assuming for this case that  $\beta = 12$ , or  $L_t = 3.78 \text{ nH}$ . The maximum error  $\delta$ ,  $W_{\max}/W_{\min}$ ,  $N_{0,\min}$ , and  $d_{\max}$  for this case are shown in Fig. 9. Compared to the FET, the maximum error and  $N_{0,\min}$  are

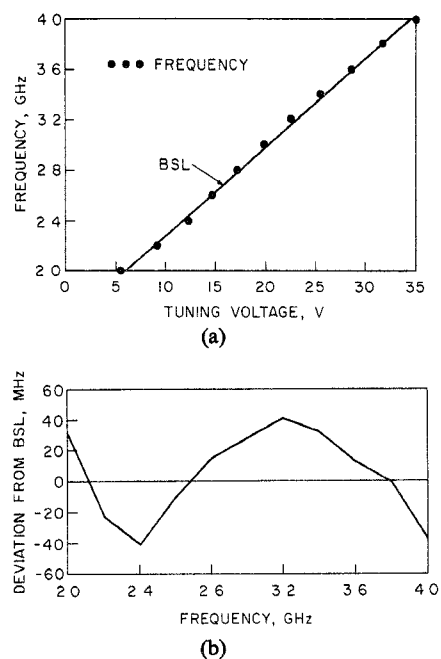


Fig. 10. (a) Tuning curve. (b) Deviation from a BSL for the BJT oscillator circuit for  $\Delta V = 30 \text{ V}$ .

several times larger, caused primarily by the large RF charge levels involved in this circuit. Also, the value of  $W_{\max}/W_{\min}$  is substantially larger, increasing the difficulty in fabricating an appropriate doping profile. If the value of  $\beta$  is increased to 16 or 20,  $\delta$  will go down only slightly while  $W_{\max}/W_{\min}$  further increases. From a tuning standpoint, the difficulties arise because the RF voltage levels across the tuning element are substantial, the fundamental component  $S_v Q_1$  being 8.5 V at 2 GHz and approximately 30 V at 4 GHz. This means that for reasonable values of  $\Delta V$ , almost the entire varactor nonlinearity is utilized at each tuning voltage, and there is not enough behavior in the given nonlinearity to obtain good tuning linearity. Nonlinearities with more degrees-of-freedom may improve the overall tuning linearity on a point-by-point basis at the expense of smoothness in the  $C(v)$  curve and doping profile. Clearly,  $n$  points could be matched exactly with an  $n$ th-order polynomial for  $f(q)$ , but the resulting  $C(v)$  curve would contain many wiggles as would the tuning curve. This is not to say that there is not a better solution for the BJT oscillator, but to find it requires an improved searching algorithm.

The tuning curve and deviation from a best straight line for the BJT oscillator with  $\Delta V = 30 \text{ V}$  are shown in Fig. 10. For this case, the peak deviation is approximately 40 MHz over the 2–4-GHz frequency range. Note that the required offset voltage to avoid forward bias is 5.5 V, while the maximum instantaneous voltage across the varactor will be 80 V. The small-signal and effective large-signal capacitance as a function of tuning voltage are indicated in Fig. 11, where substantial expansion from small to large signals is noted at the lower values of bias. Finally, the required doping profile is indicated in Fig. 12, where  $N_0 = 5.8 \times 10^{16} \text{ cm}^{-3}$ ,  $W_0 = 0.39 \mu\text{m}$ ,  $W_{\min} = 0.01 \mu\text{m}$ ,  $W_{\max} = 6.4 \mu\text{m}$ , and the device diameter is 3.9

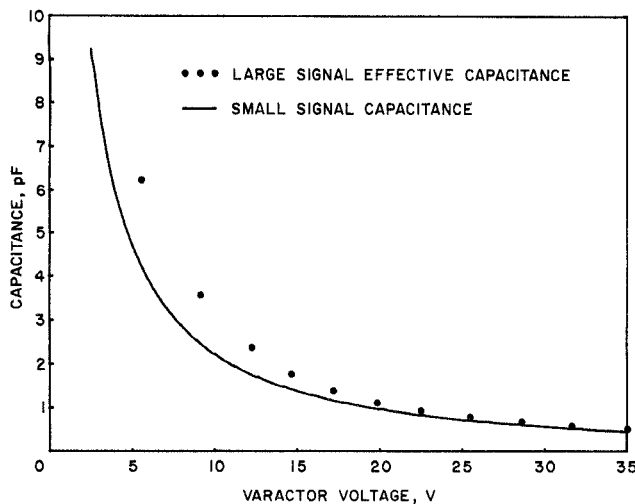


Fig. 11. Small-signal  $CV$  characteristics and effective large-signal capacitance for the BJT tuning varactor.

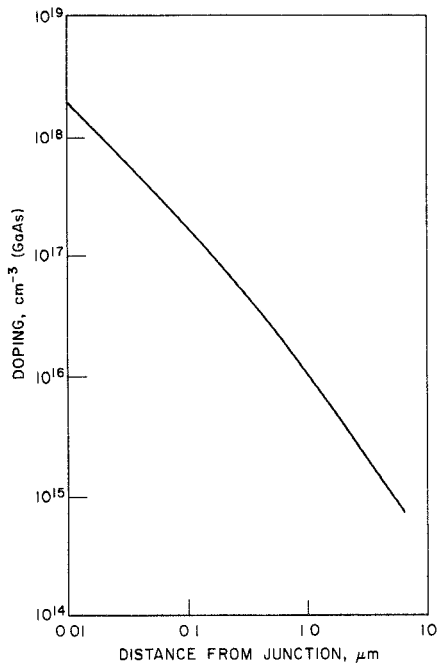


Fig. 12. Doping profile for the BJT tuning varactor having the  $CV$  characteristic of Fig. 11,  $N_0 = 5.8 \times 10^{16} \text{ cm}^{-3}$ .

mils. The variation in  $R_{s1}$  as calculated over the tuning range was  $0.2 \Omega$ . Again, because of the signal levels involved, the profile must be well controlled over a substantial distance, three orders of magnitude in  $W$ .

For a given tuning voltage range, the linearity of the BJT oscillator can be improved by perturbing  $v(q)$  in (24) with appropriate additional charge functions. In addition, even further improvements are possible by using two varactors in RF series and dc parallel, so that the RF voltage swing across each varactor is one-half as large. The results of perturbing (24) with a function  $f_1(q)$  given by

$$f_1(q) = a_1 e^{2dq} + a_2 e^{3dq} \quad (37)$$

where  $a_1$  and  $a_2$  are adjustable constants, are shown in

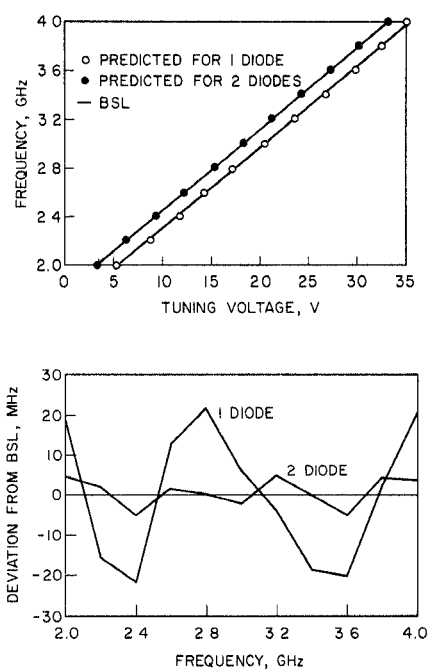


Fig. 13. (a) Tuning curves. (b) Deviation from linearity for the BJT oscillator when  $f(q)$  is perturbed by  $f_1(q)$ . Results for both a single diode and two diodes in series are shown.

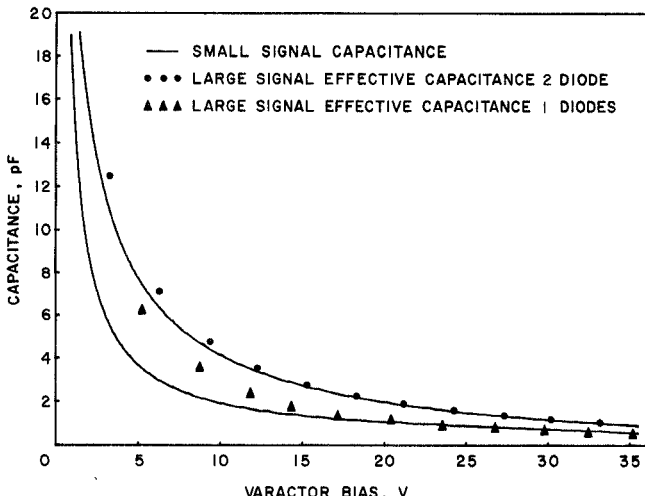


Fig. 14. Small-signal  $CV$  and large-signal effective capacitances for improved linearity tuning varactors. Results for both one and two diodes are shown for  $\Delta V = 30 \text{ V}$ .

Fig. 13 for both the one- and two-diode case. For the single diode, the deviation is reduced to 20 MHz (factor of 2) from that of Fig. 10, at the expense of more variation. When using two diodes in series, each having twice the area of the single diode while  $\beta$  remains at 12, the linearity is substantially improved to a deviation of 5 MHz. For comparison with Fig. 10 the tuning voltage range was held constant at 30 V and the single device diameter was kept at 3.9 mils. The resulting  $CV$  curves for both cases are shown in Fig. 14, and the corresponding doping profiles are indicated in Fig. 15. In the two-diode case, the profile is quite reasonable, with a  $W_{\max}/W_{\min}$  of 87, while in the single-diode case,  $W_{\max}/W_{\min} = 4700$  and the profile has a

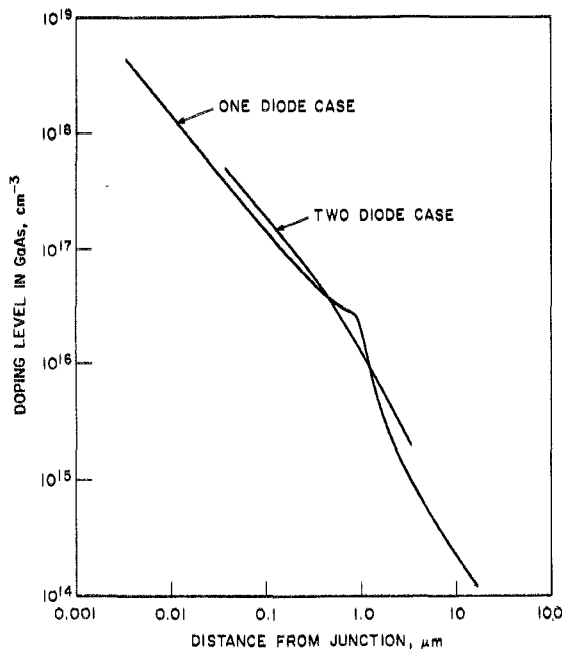


Fig. 15. Doping profiles corresponding to the  $CV$  curves of Fig. 14. The area of each diode in the two-diode case is twice that of the single-diode case.

more complicated behavior. It is clear that two diodes of twice the area in RF series and dc parallel greatly improve linearity at the expense of some additional tuning circuit complexity.

It should be noted at this point that with existing hyperabrupt tuning varactors and values of  $\Delta V$  between 10 and 20 V, BJT oscillators similar to the one in Fig. 3(b) can tune from 2 to 4 GHz with a maximum deviation of approximately 20 MHz. This occurs because the device operates forward biased over about one-half an RF cycle and the effective tuning impedance can be adjusted for tuning linearity by controlling the amount of rectification with appropriate resistance at dc. Hence the "art" of achieving tuning linearity is somewhat better than the science of predicting doping profiles. Allowing for forward bias was not part of the analysis given here because it can lead to increased oscillator post-tuning drift from trapping and thermal (varying power dissipation) effects while substantially complicating the problem. However, the effect of forward bias should be investigated further, especially if the payoff in tuning linearity is appreciable.

Attempts are presently underway to fabricate the profiles given here and other relevant profiles.

#### IV. SUMMARY AND CONCLUSIONS

A varactor profile has been identified which is capable of providing wide-band tuning linearity with an important class of microwave oscillators. These oscillators use FET's and BJT's and have simple, broad-band equivalent circuit representations and are effectively series tuned with chip varactors at a port separate from that of the output. From the comparison between an FET and BJT oscillator, it is apparent that linearity improves for realistic tuning volt-

age ranges when the RF voltage levels across the varactor are not excessive. This indicates that low-to-moderate power devices, with the resulting sacrifice in output power capability, are likely candidates for best linearity when the varactor is strictly confined to reverse bias operation. The profile obtained for the FET oscillator is reasonable and should be achievable with existing GaAs varactor fabrication technology.

#### APPENDIX

##### DERIVATION OF FOURIER COEFFICIENTS FOR THE GIVEN VARACTOR NONLINEARITY

The varactor nonlinearity in (24) can be written as

$$\frac{2cv(q)+b}{d} = \frac{1+e^{dq}}{1-e^{dq}} = \frac{2}{1-e^{dq}} - 1 \quad (A1)$$

where since  $v$  is finite,  $e^{dq} < 1$ , or  $q < 0$ . Note that  $q < 0$  is not a problem, since a constant can always be added in (22) to make the actual charge removed from the varactor positive. Because of this, then

$$\frac{1}{1-e^{dq}} = \sum_{n=0}^{\infty} e^{ndq} \quad (A2)$$

and for  $q = Q_0 + Q_1 \cos \omega t$

$$\begin{aligned} \frac{1}{1-e^{dq}} &= \sum_{n=0}^{\infty} e^{ndQ_0} e^{ndQ_1 \cos \theta} \\ &= \sum_{n=0}^{\infty} e^{ndQ_0} \left[ I_0(ndQ_1) + 2 \sum_{m=1}^{\infty} I_m(ndQ_1) \cos m\theta \right] \end{aligned} \quad (A3)$$

where the relation  $e^{A \cos \theta} = I_0(A) + 2 \sum_{m=1}^{\infty} I_m(A) \cos m\theta$  has been used, with the  $I_m(A)$  modified Bessel functions of order  $m$  and argument  $A$ . Hence, from (A3) the dc and fundamental forms can readily be obtained, i.e.,

$$\frac{2cF_0+b}{d} = 2 \sum_{n=0}^{\infty} e^{ndQ_0} I_0(ndQ_1) - 1 = 1 + 2 \sum_{n=1}^{\infty} e^{ndQ_0} I_0(ndQ_1) \quad (A4)$$

and

$$\frac{2cF_1+b}{d} = 4 \sum_{n=1}^{\infty} e^{ndQ_0} I_1(ndQ_1) \quad (A5)$$

and written as in (25).

#### ACKNOWLEDGMENT

The author would like to thank S. Booker for suggesting that two diodes may be better than one.

#### REFERENCES

- [1] D. Large, "Octave band varactor tuned Gunn diode sources," *Microwave J.*, vol. 13, p. 49, Oct. 1970.
- [2] R. A. Gough and B. H. Newton, "An integrated wide-band varactor-tuned Gunn oscillator," *IEEE Trans. Electron Devices*, vol. ED-20, pp. 863-865, Oct. 1973.
- [3] K. M. Johnson, "Wide bandwidth IMPATT and Gunn voltage tuned oscillators," in *1972 IEEE G-MTT Int. Microwave Symp. Dig. Papers*, Chicago, IL, pp. 185-186.
- [4] J. S. Joshi, "Wide-band varactor-tuned X-band Gunn oscillators in full-height waveguide cavity," *IEEE Trans. Microwave Theory Tech.*, vol. MTT-21, pp. 137-139, Mar. 1973.

- [5] B. J. Downing and F. A. Myers, "Broadband (1.95 GHz) varactor-tuning X-band Gunn oscillator," *Electron. Lett.*, vol. 7, pp. 407-409, July 1971.
- [6] M. I. Grace, "Varactor-tuned avalanche transit-time oscillator with linear tuning characteristics," *IEEE Trans. Microwave Theory Tech.*, vol. MTT-18, pp. 44-45, Jan. 1970.
- [7] C. D. Corbey, R. Davies, and R. A. Gough, "Wide-band varactor-tuned coaxial oscillators," *IEEE Trans. Microwave Theory Tech.*, vol. MTT-24, pp. 31-39, Jan. 1976.
- [8] C. S. Aitchison, "Method of improving tuning range obtained from a varactor-tuned Gunn oscillator," *Electron. Lett.*, vol. 10, pp. 94-95, Apr. 1974.
- [9] C. S. Aitchison, "Gunn oscillator electronic tuning range and reactance compensation: An experimental result at X-band," *Electron. Lett.*, vol. 10, pp. 488-489, Nov. 1974.
- [10] L. Gustafsson, G. H. B. Hansson, and K. I. Lundstrom, "On the use of describing functions in the study of nonlinear active microwave circuits," *IEEE Trans. Microwave Theory Tech.*, vol. MTT-20, pp. 402-409, June 1972.
- [11] D. F. Peterson, "Tuning speed limitations in wide-band varactor-tuned oscillators," in *1978 IEEE G-MTT Int. Microwave Symp. Dig. Papers*, Ottawa, Canada.
- [12] S. M. Sze, *Physics of Semiconductor Devices*, New York: Wiley, 1969.

# Coupled TEM Microstrip Impedance Transformer for S-Band TRAPATT Amplifiers

SIDHARTHA K. SINHA AND KENNETH P. WELLER, MEMBER, IEEE

**Abstract**—A coupled TEM microstrip line circuit suitable for use in S-band TRAPATT amplifiers has been investigated. An analytical model of the coupled-line structure has been developed which properly accounts for diode positioning on the line. This model has been used to calculate the fundamental and harmonic impedances at the device terminals for various stub terminations and device locations. Measurements made with a Hewlett-Packard network analyzer are in good agreement with the calculated results.

The use of this circuit for the development of a fixed-tuned MIC circuit for the TRAPATT amplifier on Duroid Substrate is discussed. The complete circuit incorporates a bias line filter with this coupled microstrip line and appropriate harmonic tuning stubs at two of its ports. It is capable of providing at least 6-percent 1-dB bandwidth with high efficiency and high peak power output over pulsedwidths up to 50  $\mu$ s and up to 1-percent duty cycle.

## I. INTRODUCTION

THE PERFORMANCE of microwave solid-state devices and circuitry for use as transmitter power amplifiers has been under investigation for a number of years. The TRAPATT diode is one device which has shown promise for meeting the power requirements in this application. Optimum performance of this device requires a circuit that makes it possible to achieve proper impedance loading at both the fundamental and harmonic frequencies and yet be compact and stable with temperature changes. Although TRAPATT's have been developed which can meet the power output requirements for some systems, difficulties have been encountered in meeting the bandwidth specifications [6].

Manuscript received November 27, 1978; revised April 23, 1979.  
S. K. Sinha is with Hughes Aircraft Company, Torrance Research Center, Torrance, CA 90509.

K. P. Weller was with Hughes Aircraft Company, Torrance, CA. He is now with TRW Incorporated, Defense and Space Communication Group, Redondo Beach, CA 90278.

In this paper, we shall describe a coupled TEM circuit in microstrip that appropriately takes into account the positioning of the device anywhere on the line and accommodates any arbitrary terminations at the ends of the coupled line. This circuit model gives insight into the problem of bandwidth limitation in a TRAPATT amplifier, and has helped in developing an approach for improvement of bandwidth. The circuit developed has been used with TRAPATT diodes bonded on diamond heat sinks to obtain jitter-free pulsed-power outputs up to 50 W with 22-percent efficiency, 6-dB gain, and a 6-percent 1-dB bandwidth from a single device operated with a 50- $\mu$ s wide pulse and up to 1-percent duty factor. The circuit developed has no lumped tuning capacitors unlike the earlier works [7], [8], and can be used to obtain good performance from a variety of devices with no circuit tuning.

## II. CIRCUIT CHARACTERIZATION

### A. Physical Description

In its simplest form, the circuit consists of two coupled lines in a microstrip configuration operating in a quasi-TEM mode. The basic structure of the circuit is shown in Fig. 1. The line is approximately a quarter wavelength long at center frequency. The TRAPATT diode is mounted approximately one-third of the linelength from one end. In an actual amplifier circuit, the bias line filter is connected between the end of the line and the location of the diode, and a suitable resonant tuning stub to improve the bandwidth of the amplifier is printed at the other end of the line. Also the output line in an actual amplifier circuit may have a third-harmonic tuning stub.